ZANCO Journal of Pure and Applied Sciences
The official scientific journal of Salahaddin University-Erbil
https://zancojournals.su.edu.krd/index.php/JPAS

**ISSN (print ):**2218-0230**, ISSN (online):** 2412-3986**, DOI:** http://dx.doi.org/10.21271/zjpas

RESEARCH PAPER

# Kinetic studies of copper-catalyzed homocoupling reactions of arylboronic acids in aqueous micellar media

Hawta K. Abdullah[1], Mazin A. Othman[1]
[1]Department of Chemistry ,College of Science, Salahaddin University-Erbil, Kurdistan Region, Iraq .

**A B S T R A C T:**
The kinetic studies for copper-catalyzed homocoupling of some phenylboronic acids have been successfully carried out in an aqueous micellar medium under environmentally benign conditions (water as a solvent, micelle to help solubilize hydrophobic adducts). In this study cetyl trimethyl ammonium bromide (CTAB ) is used as a surfactant to produce micelle. Different copper salts and copper complexes were used as catalysts to perform the reaction under the mild condition at a temperature range (40-65˚C, under air) without the addition of any additives (base, oxidant, and ligands). The reactions were followed using a UV-Vis spectrophotometer and the absorbances were measured at maximum wavelengths for the biphenyl production of each of five selected phenylboronic acids. The observed rate constants ($k_{obs}$) were calculated using a pseudo-first-order equation and unsubstituted phenylboronic acid was selected for optimization processes. The experimental results showed good to excellent curve fit ($R^2$=0.9967-0.9998) to the pseudo-first-order equation and origin software was used for this purpose. Among all copper catalysts, the observed rate constant ($k_{obs}$) for cupric acetate ($Cu(OAc)_2$)is much higher than others, ($k_{obs}$=0.1605 $min^{-1}$), while $CuCl_2.2H_2O$ has a minimum observed rate constant, $k_{obs}$=0.0216$min^{-1}$. The two copper complexes [Cu(4-mba)$_2$(tmeda)], and [Cu(3-mba)$_2$($H_2O$)$_2$(tmeda)] (4-mbaH = 4-methylbenzoic acid, 3-mbaH = 3-methylbenzoic acid, tmeda = *N,N,N',N'* - tetramethylethyleneamine) require a mild condition (85˚C) which is higher than other copper catalysts when unsubstituted phenylboronic acid is used as reactant the value of $k_{obs}$ is (0.0176, 0.0343 $min^{-1}$) respectively, while using *p*-tolylboronic acid (**1b**) as reactant the value of $k_{obs}$ is (0.0173, 0.0147 $min^{-1}$) respectively.

KEY WORDS: homocoupling, phenylboronic acids, biphenyls, cetyl trimethyl ammonium bromide (CTAB) .
DOI: http://dx.doi.org/10.21271/ZJPAS.34.6.21
ZJPAS (2022) , 34(6);184-204 .

## 1.INTRODUCTION :

C–C bond formation reactions are a major strategy for constructing important building blocks in organic synthesis (Miyaura and Suzuki, 1995, Horton et al., 2003, Lloyd-Williams and Giralt, 2001). Biphenyls are a class of organic compounds found in a wide range of natural products, with uses in pharmaceuticals, agrochemicals, dyes, semi-conductors, and asymmetric synthesis (Corbet and Mignani, 2006, Khalily et al., 2012, Monnier and Taillefer, 2009, Karimi and Akhavan, 2009, Martin and Buchwald, 2008). The development of simple and ecologically friendly reactions for the synthesis of biphenyls is still a hot topic of research. Transition-metal-catalyzed couplings, such as the Suzuki reaction, have made significant advances in the synthesis of symmetrical and unsymmetrical biphenyls (Marion et al., 2006, McGlacken and Bateman, 2009). The Pd(II)-catalyzed homocoupling of boronic acids has been widely researched (Jin et al., 2009, Mitsudo et al., 2009, Mu et al., 2009, Amatore et al., 2008, Cicco et al., 2010, Mitsudo et al., 2008, Prastaro et al., 2010). The kinetics of palladium-catalyzed aerobic oxidative homocoupling reaction of phenylboronic acids in an aqueous micellar medium (Othman, 2011). The stability of the Pd(II)-*β*-CD catalyst and its catalytic activity in the aerobic homocoupling reaction of phenylboronic acid were investigated (Othman, 2020). These catalytic techniques, however, have some limits, such as (i) Palladium is costly, and additional ligands are frequently needed (Jin et al., 2009, Zhou et al., 2007, Yamamoto, 2007, Yamamoto et al., 2006), (ii)

* Corresponding Author:
Mazin A. Othman
E-mail: mazin.othman@su.edu.krd
**Article History:**
Received: 22/06/2022
Accepted: 09/08/2022
Published: 20/12 /2022

certain oxidants are employed to restore the catalyst (Amatore et al., 2008, Cheng et al., 2007, Mitsudo et al., 2009, Kabalka and Wang, 2002, Parrish et al., 2002, Klingensmith and Leadbeater, 2003, Mitsudo et al., 2008), (iii) to obtain high yields of biphenyls, a strong base must be added (Wong and Zhang, 2001, Jin et al., 2009, Yadav et al., 2007, Burns et al., 2007) and (iv) to complete the reaction high temperature is needed (Amatore et al., 2008, Cheng et al., 2007, Prastaro et al., 2010). Copper has recently been discovered to be a low-cost, environmentally friendly metal catalyst for the production of useful organic compounds. CuI-catalyzed coupling of alkyl boron reagents with phenyl and heterophenyl iodides results in high yields of coupled products (Basnet et al., 2016). We have selected some phenylboronic acids (Scheme 1(a)) to perform this reaction using different copper catalysts which accordingly lead to the production of different biphenyls (Scheme 1(b)).

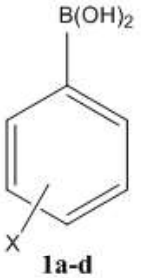


**1a-d**

**(a)**

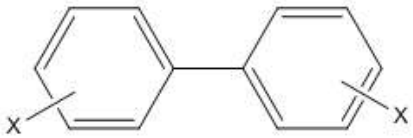


**2a-d**

**(b)**

**Scheme 1. (a) 1a** X=H(phenylboronic acid), **1b** X=4-$CH_3$(*p*-tolylboronic acid), **1c** X=4-$COCH_3$(4-acetylphenylboronic acid), **1d** X=COH(4-Formylphenylboronic acid), **(b) 2a** X=H(biphenyl), **2b** X=4-$CH_3$(4,4'-dimethyl-1,1'-biphenyl), **2c** X=4-$COCH_3$(1,1'-([1,1'-biphenyl]-4,4'-diyl)bis(ethan-1-one), **2d** X=COH([1,1'-biphenyl]-4,4'-dicarbaldehyde).

Previous researches show that certain copper species can be used to mediate the homocoupling of **(1a-d)**. Cupric acetate ($Cu(OAc)_2$) can promote the homocoupling of phenylboronic acids for the production of biphenyls, according to Demir and co-workers. (Demir et al., 2003). Yamamoto et al. developed an effective approach for obtaining symmetrical biphenyls in the air by homocoupling phenylboronic acids catalyzed by 1,10-phenanthroline-ligated copper complexes, however when electron-withdrawing functionalities are employed as phenylboronic acids, yields are low, (Kirai and Yamamoto, 2009). The homocoupling of phenylboronic acids could be mediated by cheap copper(II) sulfate, according to Kaboudin and co-workers. This approach necessitates the use of a stoichiometric quantity of $CuSO_4$ and heating in difficult-to-handle DMF. A catalytic cycle including three basic stages is thought to be involved in the homocoupling of phenylboronic acid. (1) oxidation (2)transmetalation, and (3) reductive elimination as shown in **(Scheme 2)**.

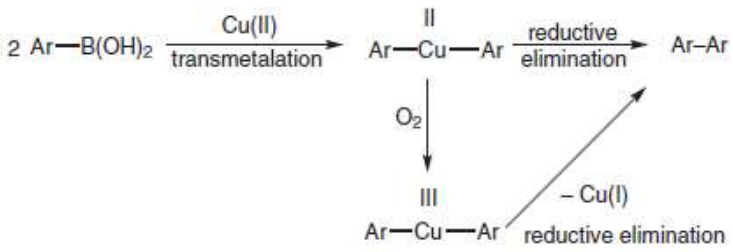


**Scheme 2.** A plausible mechanism for the homocoupling of **1a**. (Kaboudin et al., 2011b).

In addition, Kaboudin and collaborators discovered that the ($Cu_2$–β-CD) complex is an excellent dinuclear supramolecular nanoreactor catalyst for phenylboronic acid coupling reactions in the air under ligand- and base-free conditions (Kaboudin et al., 2011a). Singh and a group of researchers discovered phenylboronic acid homocoupling catalyzed by clay encapsulated Cu(OH)x (Dar et al., 2014). According to Puthiaraj and colleagues, copper terephthalate Cu(BDC) metal-organic framework MOF can be used as an efficient heterogeneous reusable catalyst for aerobic homocoupling of phenylboronic acids while maintaining the Cu(BDC) MOF's crystallinity and structure (Puthiaraj et al., 2014). Raul et.al. demonstrated a simple and effective hetero nano CuO catalyzed homocoupling reaction of phenylboronic acids for the production of symmetrical biphenyls throughout a moderate environment without using additives (Raul et al., 2015). Parshamoni and collaborator's developed a copper(I)-based 2D MOF, namely, [[$Cu_2Br_2$(pypz)]n·n$H_2O$] (Cu-Br-MOF) [pypz=bis[3,5-dimethyl-4-(4'-pyridyl)pyrazol-1-yl] methane] by using a flexible pypz bridging ligand. In Cu-Br-MOF, the copper ions are four coordinated and have a tetrahedral geometry, and this proves to act as a heterogeneous catalyst for the aerobic homocoupling of phenylboronic acids and the epoxidation of olefins. (Parshamoni et al., 2016). CuCl-catalyzed homocoupling of phenylboronic acids in the air at ambient temperature was reported by Cheng and Luo. Biphenyls could be made in three hours without applying any chemicals and with an average yield of less than 80% employing this approach. Bases have been discovered to inhibit homocoupling (Cheng and Luo, 2011). At ambient temperature, Cao and co-workers described a ligand-free $CuCl_2$•2$H_2O$-catalyzed homocoupling reaction of (het)phenylboronic acids (Cao et al., 2017). The establishment of homocoupling conditions for (hetero)phenylboronic acids utilizing a cheap and easily accessible copper catalyst and 2-O-Methyl-d-Glucopyranose (2-OMG) were reported. These reactions were performed at low temperatures with high yields, using substituted phenylboronic acids and cheap Cu(II) acetate (Yuan et al., 2019). Yang et. al. have developed a copper-based MOF catalyzing the aerobic homocoupling of phenylboronic acids to biphenyls using the L-$NO_2$ ligand (Yang et al., 2021b). Pourmorteza and co-workers have synthesized $TiO_2$–ascorbic acid (AA)–Cu(II), nanohybrid and used it as an effective catalyst for the oxidative homocoupling of phenylboronic acids under air using visible light in tetrahydrofuran (THF) at room temperature (Pourmorteza et al., 2022). Copper-based MOF (1) catalyzes the aerobic homocoupling of phenylboronic acids to biphenyls which are constructed by the L-$NO_2$ ligand **(Scheme 3)**.

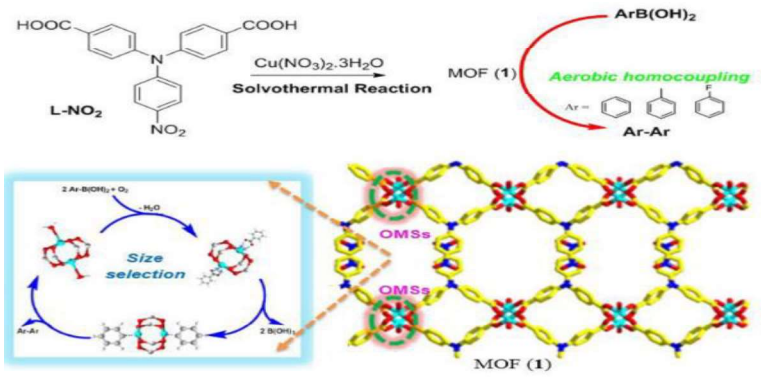


**Scheme 3**. Aerobic homocoupling reaction of phenylboronic acids mediated by MOF (1) (Yang et al., 2021a)

This paper aimed to explore the kinetics of the homocoupling reaction of (**1a)**s in an aqueous micellar medium under environmentally benign conditions (water as a solvent), as it is typically cheap and plentiful, non-flammable, non-toxic, and has a relatively low environmental impact (especially compared to dimethylformamide (DMF) or toluene, which are more typically used in palladium-catalyzed coupling reactions) (Bouleghlimat et al., 2017) and (micelle to help solubilize hydrophobic adducts) in this study CTAB (cetyl trimethyl ammonium bromide) is used as surfactant to produce micelle **(Scheme 4)**.

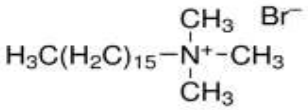

**Scheme 4**. Cetyltrimethylammonium bromide (CTAB) (Gratzel, 2020).

Micelles are spherical supramolecules that are generated by amphiphiles in water or media that are comparable to water (Scheme 5). Because the aggregates are colloidal in size, a micellar system seems to be homogenous; nonetheless, the absorbed reactants are in a micro-heterogeneous two-phase system (Gratzel, 2020).

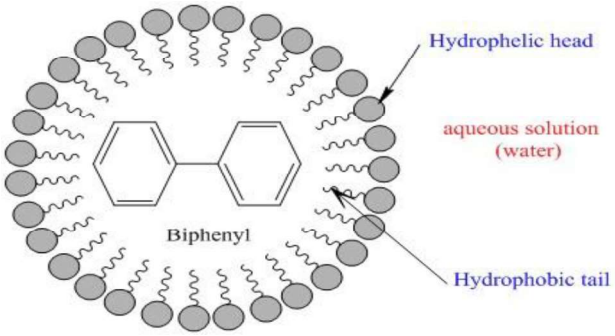


**Scheme 5**. spherical micelle formed to solubilize the product (biphenyl)of homocoupling reaction of **1a-d** using copper as a catalyst.

When it comes to the acceleration of the rate of a reaction, the micellar effect is described as "micellar catalysis" in general; nevertheless, this assignment is merely an assumption for a kinetic study (Scrimin et al., 1998). Because the reaction is copper-catalyzed, our first task is to select a good catalyst to obtain accurate and repeatable kinetic results.

## 2. Experimental

### 2.1. Equipment

A UV-visible spectrophotometer (Shimadzu-UV-1900i) was used for monitoring the reactions. The temperature of the reaction is controlled using a circulating water bath system with a cell holder which was homemade.

### 2.2. Chemicals

All chemicals were purchased from commercial resources (Sigma-Aldrich) and used without further purification. The two copper complexes ([Cu(4-mba)$_2$(tmeda)] and [Cu(3-mba)$_2$(H$_2$O)$_2$(tmeda)] were prepared by a group of researchers (Kansız et al., 2021). Distilled water and ethanol were used for preparing stock solutions of **1a-d**. As well as ethanol was used to prepare copper complexes.

### 2.3. Time-resolved absorption peak measurements

All the kinetic studies for the reactions were carried out in 1.00 cm path length stoppered quartz cuvettes (Hellma) (3 ml) at 40˚C. A typical concentration of (**1a and 1b**) was $6\times10^{-4}$ mol $L^{-1}$ **(1c and 1d)** $6\times10^{-5}$ mol $L^{-1}$, with a needed amount of catalyst. Product formation (biphenyl) was followed through the change in UV-Visible

absorbance with time at a selected wavelength where maximum changes in absorbance occurred, which has been selected through UV-Visible time-resolved absorption spectra measurement for the reaction of each phenylboronic acid **(**276 nm for **2a,** 279 nm for **2b** and **2c,** and 282 nm for **2d)**. The essential reagents (CTAB, and catalyst) were mixed by pipetting the required quantity from the concentrated stock solutions into a 1.0 cm pathlength cuvette with a total volume of 3 mL. The cuvette was allowed to equilibrate thermally for 5 minutes. Then the required concentration of **1a-d** was added to the cuvette from the concentrated stock solution. Finally, for the kinetic studies, the absorbance at maximum wavelength was taken for all reactions. The analysis of the data and the kinetics curve fits done using origin program software (Origin 2018).

## 3. Result and discussion:

UV-Visible spectroscopy was used to track the homocoupling reactions of **1a-d** to produce **2a-d** by measuring the absorbance of the reaction mixture at various wavelengths which have the maximum absorbance versus time ($\lambda_{max}$) (**Scheme 6**).

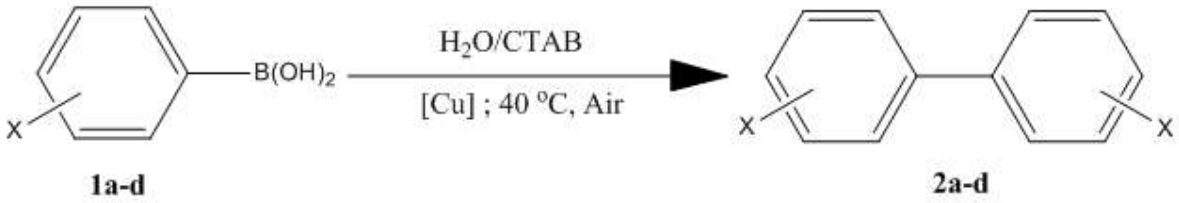


**1a-d** **2a-d**

**Scheme 6**

### 3.1. Maximum wavelength selection for the reaction

Before the optimization process, the maximum absorbance at the selected wavelength is determined by taking the homocoupling of **1a**, we performed the reaction using $6\times10^{-4}$ mol $L^{-1}$ of **1a** in $1.1\times10^{-2}$ mol $L^{-1}$ CTAB using $1.8\times10^{-3}$ mol $L^{-1}$ concentration of $(Cu(OAc)_2)$ as a catalyst at 65˚C (Figure 1).

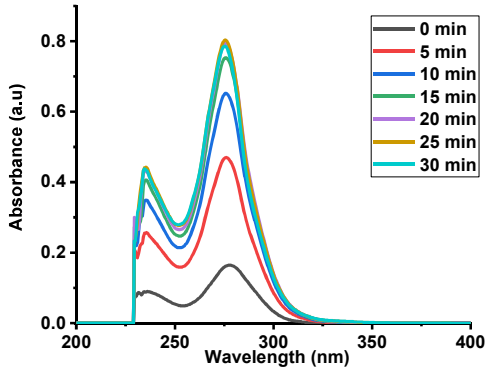


**Figure 1**. Time-resolved absorption peaks for the reaction of $6\times10^{-4}$ mol $L^{-1}$ **1a** in $1.1\times10^{-2}$ mol $L^{-1}$ CTAB using $1.8\times10^{-3}$ mol $L^{-1}$ $Cu(OAc)_2$ at 65˚C.

The reaction showed that there is an increase in absorbance as a function of time at 276 nm when the absorbance is at its maximum value ($\lambda_{max}$), this explains the product formation. According to Beer lambert's law, there is a direct relation between absorbance and concentration which means that as the reaction proceed the product concentration increases. Hence, the absorbance increased at 276 nm is for the product (biphenyl) formation in the case of **1a**. Accordingly, the $\lambda_{max}$ for the reaction of all other studied phenylboronic acids **1b-d** were determined (vide supra) (Atkins et al., 2014). The maxium wavelength ($\lambda_{max}$ ) of 276 nm was selected for all kinetic data in optimization processes using **1a**.

### 3.2. Effect of surfactant concentration on the reaction rate

The concentration of added surfactant was discovered to have a significant effect on the reaction rate. Fixing wavelength at 276 nm the effect of CTAB concentration was studied using different concentrations of CTAB as shown in (Figure 2).

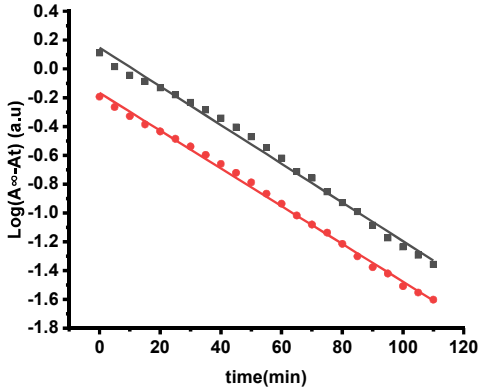


**Figure 2**. Pseudo-first-order kinetic plots for the reaction of $6\times10^{-4}$ mol $L^{-1}$ **1a** in **(●)** $9\times10^{-3}$ mol $L^{-1}$, **(■)** $1\times10^{-2}$ mol $L^{-1}$ CTAB using $1.8\times10^{-3}$ mol $L^{-1}$ $Cu(OAc)_2$ at 40˚C, Experimental data (dotted line), solid line fit to the (pseudo) first-order equation (1), $k_{obs}$ = (0.0301, and 0.0309 $min^{-1}$) respectively.

As shown in **Figures 2 (a),** and **(b)** the reaction shows linear relation according to the pseudo-first-order equation (1).

$$\mathrm{Log}(A_\infty - A_t) = \log A_\infty - \frac{kt}{2.303} \quad \text{---------(1)}$$

(Atkins et al., 2014)

Where: $A_t$ Absorbance at the time (t), $A_\infty$: Absorbance at the time ($t_\infty$), t: time in minutes, k: rate constant ($min^{-1}$). By plotting $\mathrm{Log}(A_\infty - A_t)$ versus time (min) the slope is equal to $\left(-\frac{k}{2.303}\right)$.

As the curve fitting obeys **(equation.1)** therefore the reaction is pseudo-first-order kinetics with $(k_{obs} = -\mathrm{slope} \times 2.303)$.

The calculated $k_{obs}$ were plotted against CTAB concentration **Figure 2.1**.

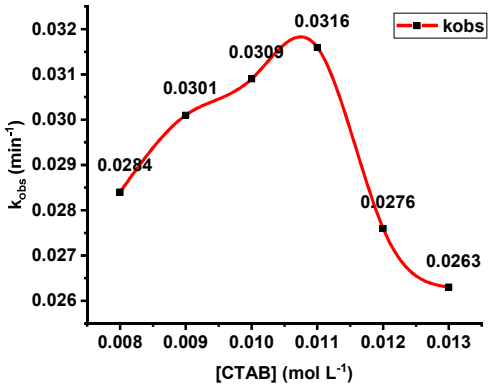


**Figure 2.1**. Effect of CTAB concentration on the $k_{obs}$ for the reaction involving $6\times10^{-4}$ mol $L^{-1}$ **1a** (■), using $1.8\times10^{-3}$ mol $L^{-1}$ $Cu(OAc)_2$ at 40˚C

**Figure 2.1** shows that increasing surfactant concentration has a rate-enhancing effect, which declines at high surfactant concentration and this is typical in micellar solutions. The reactants are brought together in the micelles, which causes a rise in $k_{obs}$ at first. Dilution of reactant molecules over increasing numbers of micelles with increasing surfactant concentration results in a

drop in $k_{obs}$ (Buurma, 2009). The observed rate constant increase as the concentration of CTAB increases until reaches critical micelle concentration (CMC) (The CMC: is the lowest concentration at which spherical micelles form ) (van Os et al., 2012) but when exceeds CMC starts to decline. The CMC of CTAB is $1\times10^{-2}$ mol $L^{-1}$ in our study the optimum condition for CTAB concentration was $1.1\times10^{-2}$ mol $L^{-1}$

### 3.3. Effect of catalyst concentration on the reaction rate:

We investigated the effect of catalyst concentration $Cu(OAc)_2$ on the observed rate constant for the homocoupling reaction of **1a** at our optimum condition **Figure 2.2**.

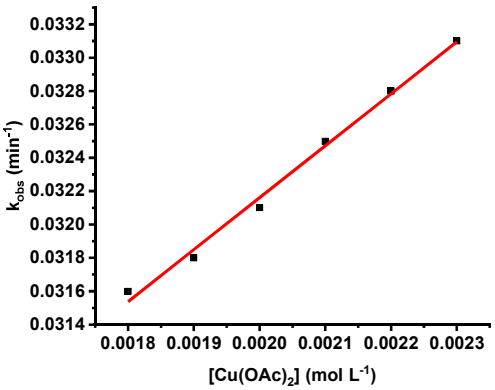


**Figure 2.2**. Effect of concentration of $Cu(OAc)_2$ on $k_{obs}$ for the reaction involving $6\times10^{-4}$ mol $L^{-1}$ **1a**, in $1.1\times10^{-2}$ mol $L^{-1}$ CTAB at 40˚C, Experimental data (dotted line), solid line fit to the (pseudo) first-order equation (1).

**Figure 2.2** shows that the reaction is first order in the catalyst, as expected based on the assumption that there is only one catalyst molecule involved in the catalytic cycle. At elevated concentration, there will be more $Cu(OAc)_2$ molecules in the catalytic cycle therefore $k_{obs}$ increase.

### 3.4. Effect of 1a concentration on the reaction rate:

To further study the order of the reaction in **1a**, we studied the effect of **1a** concentration on the reaction rate in $1.1\times10^{-2}$ mol $L^{-1}$ CTAB using ($2\times10^{-3}$ mol $L^{-1}$) $Cu(OAc)_2$ at 40˚C as shown in **Figure 2.3**.

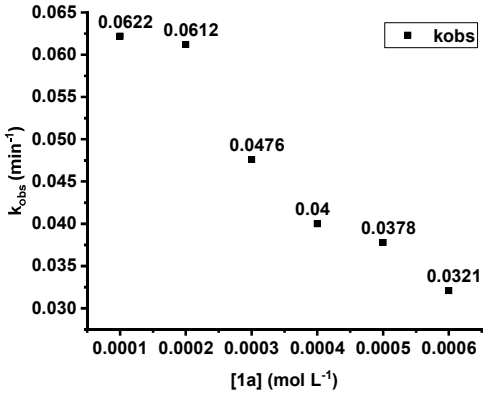


**Figure 2.3**. Effect of **1a** concentration on the observed reaction rate constant $k_{obs}$(■), in $1.1\times10^{-2}$ mol $L^{-1}$ CTAB, using $2\times10^{-3}$ mol $L^{-1}$ of $Cu(OAc)_2$, at 40˚C.

**Figure 2.3** shows that the observed pseudo-first-order rate constant lowers as the concentration of **1a** increases. Many variables could be responsible for the drop in the observed rate constant when the **1a** concentration rises. First, to begin with, a decrease in $O_2$ concentration throughout the

reaction could explain the decline in the rate constant with increasing **1a** concentration. Second, **1a** has the potential to dimerize or trimerize (Gallon et al., 2007). (**1a**)s concentration dependency is reversed kinetically **1a** dimerization and trimerization are most probable to appear in the micelles' hydrophobic region (core) **(Scheme 7)**.

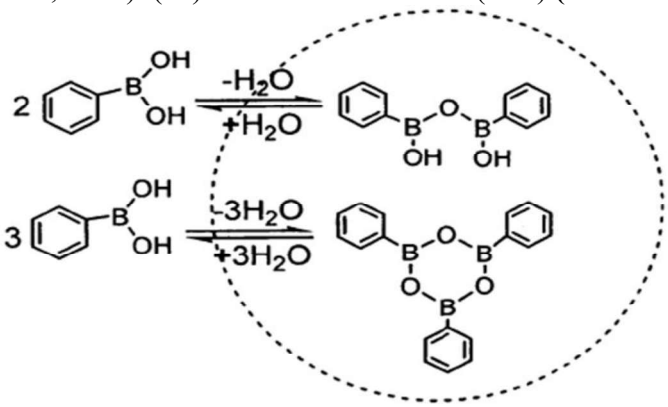


**Scheme 7.** Dimerization and trimerization of phenylboronic acid

These dimers and/or trimers, however, hydrolyze rapidly to the proper **1a** in aqueous environments. As a consequence of the micelles' extremely dynamic structure (Prastaro et al., 2009). Continuously, these dimers and/or trimers will be generated and hydrolyzed. As the concentration of **1a** increases, the possibility for dimer and/or trimer formation increases, which could be one of the causes for the decrease in kobs. Third, the effect of added cetyltrimethylammonium bromide (CTAB) on the reaction varies greatly depending on the **1a** concentration used, showing that **1a** distribution throughout the aqueous and micellar pseudo phases is the source of kinetic complexity.

**3.5. Effect of temperature on the reaction rate:**
The reaction has been done by controlling the temperature in the range of 40-65˚C the following results are obtained in **Figure 2.4**.

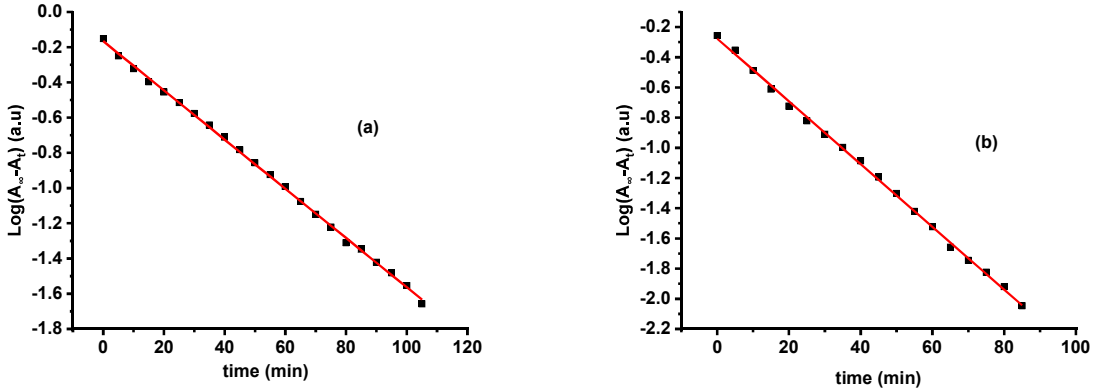


**Figure 2.4.** Pseudo first-order kinetic plots for the reaction of $6\times10^{-4}$ mol $L^{-1}$ **1a** in $1.1\times10^{-2}$ mol $L^{-1}$ CTAB using $2\times10^{-3}$ mol $L^{-1}$ $Cu(OAc)_2$ at **(a)** 40˚C, **(b)** 45˚C Experimental data (dotted line), solid line fit to the (pseudo) first-order equation (1), $k_{obs}$ = (0.0321, and 0.0478 $min^{-1}$) respectively.

**Figure 2.4.** shows that with increasing the temperature of reaction the $k_{obs}$ is increased means that directly proportional.

The Arrhenius activation energy is calculated by measuring rate constants at various temperatures and is applicable for most homogenous and complex reactions. From the Arrhenius equation **(equation.2)** the rate of reactions is increased exponentially with increasing absolute temperature (Marin, 2011).

$k = Ae^{\frac{Ea}{RT}}$ ---- 2) (Atkins et al., 2014)

By taking (log) for **(equation.2)** we get **(equation.2.1)**

$$\text{Logk} = \text{logA} - \frac{\text{Ea}}{2.303\text{RT}} \text{----------(2.1)}$$

Where : k: rate constant ($min^{-1}$), A: Arrhenius pre-exponential factor, Ea: Arrhenius activation energy, R: is the gas constant (1.987 cal $mol^{-1}$ $K^{-1}$ or 8.314 J $mol^{-1}$ $K^{-1}$), T: is the absolute temperature. By plotting Log $k_{obs}$ ($min^{-1}$) versus $\left(\frac{1}{T}(K^{-1})\right)$the slope equal to $(\frac{-Ea}{2.303R})$. Therefore from **Figure 2.5**, the calculated activation energy is Ea = 15.655 Kcal

The rate of reaction usually increases when the temperature rises. The average kinetic energy of the reactant molecules will grow as the temperature rises. As a result, a higher percentage of molecules will have the minimum activation energy required for a successful collision (Atkins et al., 2014). As in our reaction higher temperature cause faster collision between **1a** molecules and Cu-catalyst molecule as a result $k_{obs}$ will increase. By taking the $\log k_{obs}$ versus $\frac{1}{T}K^{-1}$ we get **Figure 2.5**.

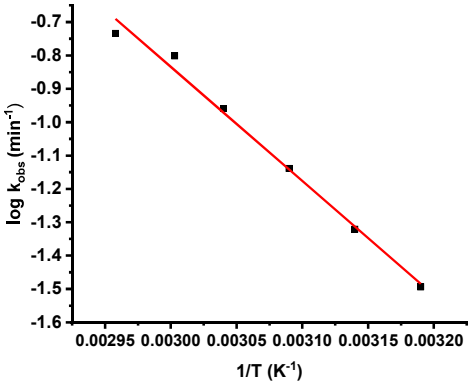


**Figure 2.5**. Effect of temperature on $k_{obs}$ for the reaction involving $6\times10^{-4}$ mol $L^{-1}$ **1a**, in $1.1\times10^{-2}$ mol $L^{-1}$ CTAB using $Cu(OAc)_2$ at the temperature range of 40-65˚C, Experimental data (dotted line), solid line fit to the (pseudo) first-order equation (1).

### 3.6. Homocoupling of (1a)s using different Cu(molecular and complex) catalysts.

After the optimization process has been done the homocoupling reaction is done under optimized conditions.

### 3.6.1: Homocoupling of 1a using different Copper(molecular and complex) catalysts.

The homocoupling reaction of **1a** is done under optimized conditions.

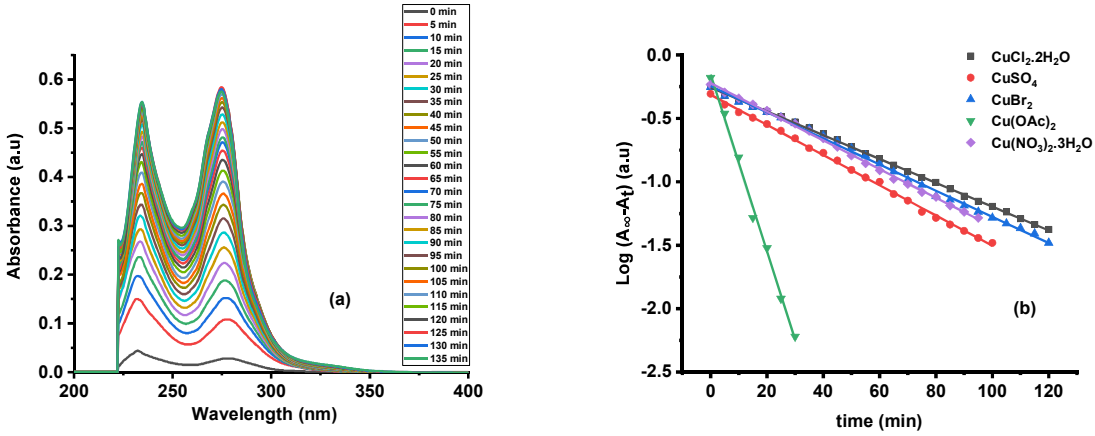


**Figure 2.6**. **(a)** Time-resolved absorption peaks, **(b)** Pseudo first-order kinetic plots for the reaction of $6\times10^{-4}$ mol $L^{-1}$ **1a** in $1.1\times10^{-2}$ mol $L^{-1}$ CTAB using $1.8\times10^{-3}$ mol $L^{-1}$ of (■) $CuCl_2.2H_2O$, (●) $CuSO_4$, (▲) $CuBr_2$, (▼) $Cu(OAc)_2$ and (♦) $Cu(NO_3)_2.3H_2O$, Experimental data (dotted line), solid line fit to the (pseudo) first-order equation (1), at 65˚C

**Figure 2.6 (a)** shows that there is increasing in absorbance at 277nm for **(b-f)** as the reaction proceeds the **2a** is produced as the only product without phenol. The selection of temperature range (40-65˚C) was not arbitrary since the used Cu-catalysts solutions have pale blue colors which can absorb light near the UV region the absorbances of the reaction mixture move out of scale when we use high concentration Cu-catalysts therefore the temperature raised and lower Cu-catalysts concentration was used to overcome this problem. The observed rate constant $k_{obs}$ for the **Figure 2.6** is shown in **Table 1**.

**Table 1.** The observed rate constant $k_{obs}$ for the reaction of **1a** at optimum conditions using different copper catalysts.

| 1a (mol $L^{-1}$) | Cu-catalysts ($1.8\times10^{-3}$ mol $L^{-1}$) | $k_{obs}$ ($min^{-1}$) |
|---|---|---|
| $6\times10^{-4}$ | $Cu(OAc)_2$ | 0.1605 |
| $6\times10^{-4}$ | $CuSO_4$ | 0.0274 |
| $6\times10^{-4}$ | $Cu(NO_3)_2.3H_2O$ | 0.0260 |
| $6\times10^{-4}$ | $CuBr_2$ | 0.0237 |
| $6\times10^{-4}$ | $CuCl_2.2H_2O$ | 0.0216 |

### 3.6.2: Homocoupling of 1a using different Copper complex catalysts.

The homocoupling reaction of **1a** is done under mild temperature conditions for (a and b) complexes (**Figure 2.7**).

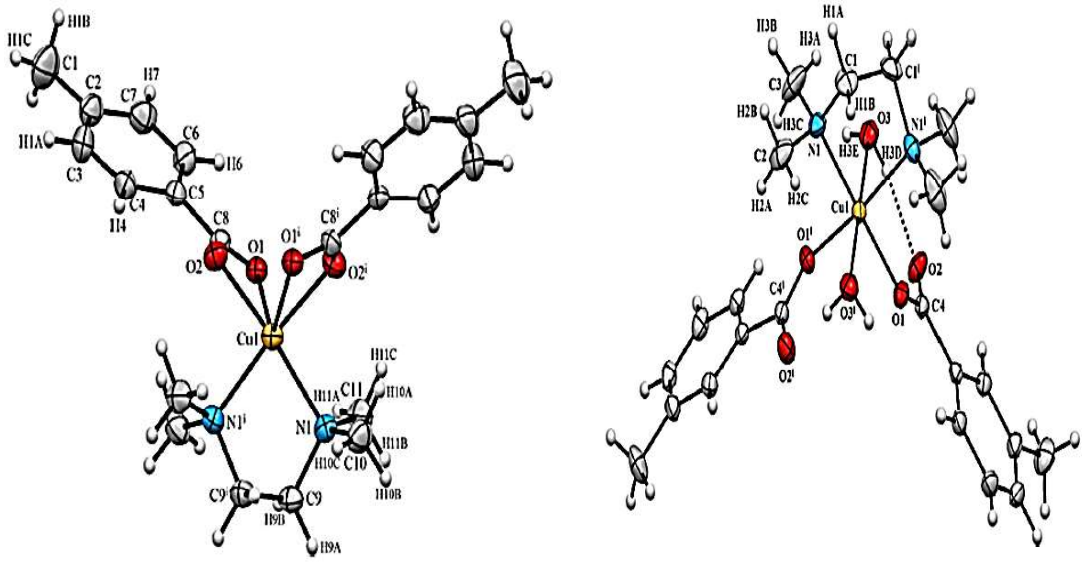

**(a)** **(b)**

**Figure 2.7**. **(a)** $[Cu(4\text{-mba})_2(tmeda)]$ and **(b)** $[Cu(3\text{-mba})_2(H_2O)_2(tmeda)]$ (Kansız et al., 2021)

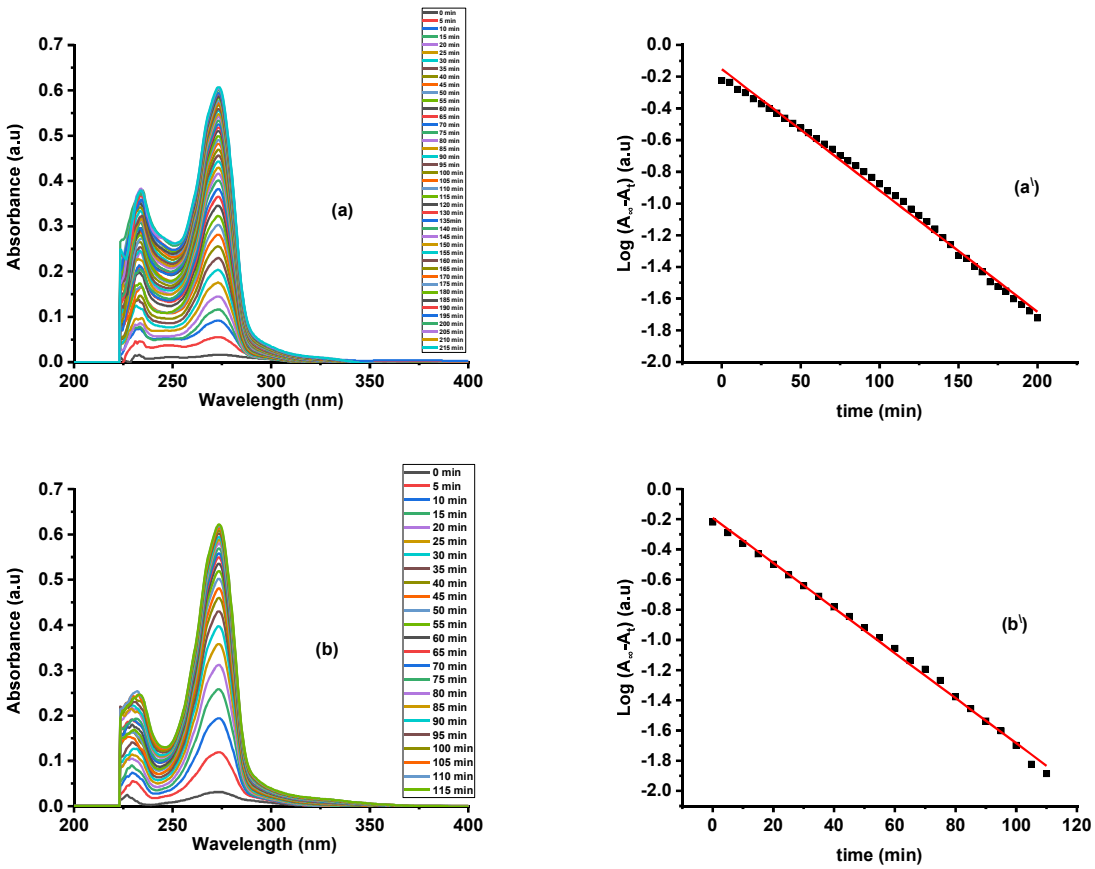


**Figure 2.8**. **(a,b)** Time-resolved absorption peaks, **(a',b')** Pseudo first-order kinetic plots for the reaction of $6\times10^{-4}$ mol $L^{-1}$ **1a** in $1.1\times10^{-2}$ mol $L^{-1}$ CTAB using $8\times10^{-5}$ mol $L^{-1}$ of **(a)** [Cu(4-mba)$_2$(tmeda)] and **(b)** [Cu(3-mba)$_2$($H_2O$)$_2$(tmeda)], **(a',b')** Experimental data (dotted line), solid line fit to the (pseudo) first-order equation (1), at 85˚C, $k_{obs}$=(0.0176, 0.0343 $min^{-1}$) respectively.

**Figure 2.8.** shows that there is increasing in absorbance for **(a)** [Cu(4-mba)$_2$(tmeda)] and **(b)** [Cu(3-mba)$_2$($H_2O$)$_2$(tmeda)] at 273nm where the absorbance has the highest value.

### 3.7.1: Homocoupling of *p*-tolylboronic acid (1b) using different copper catalysts.

Under optimized conditions, the homocoupling reaction of **1b** using a different copper catalyst (a-e) is done. **Figure 2.9**.

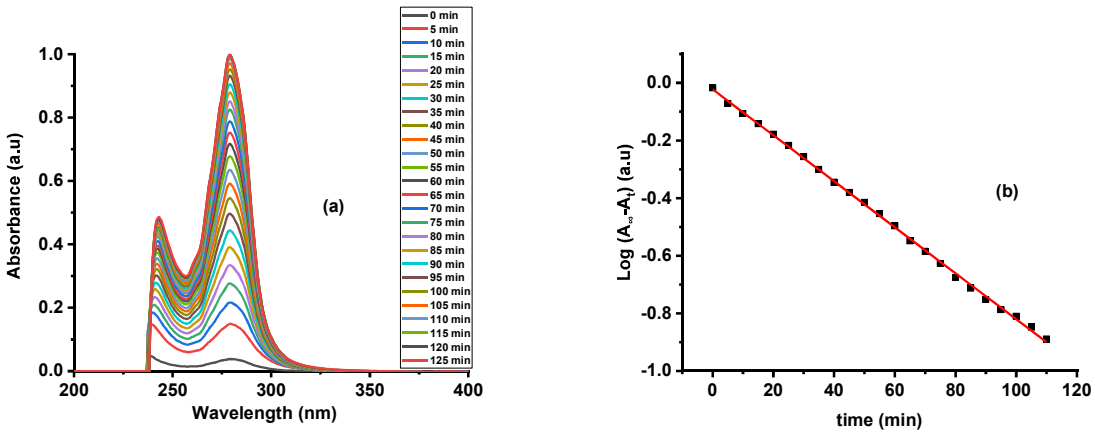

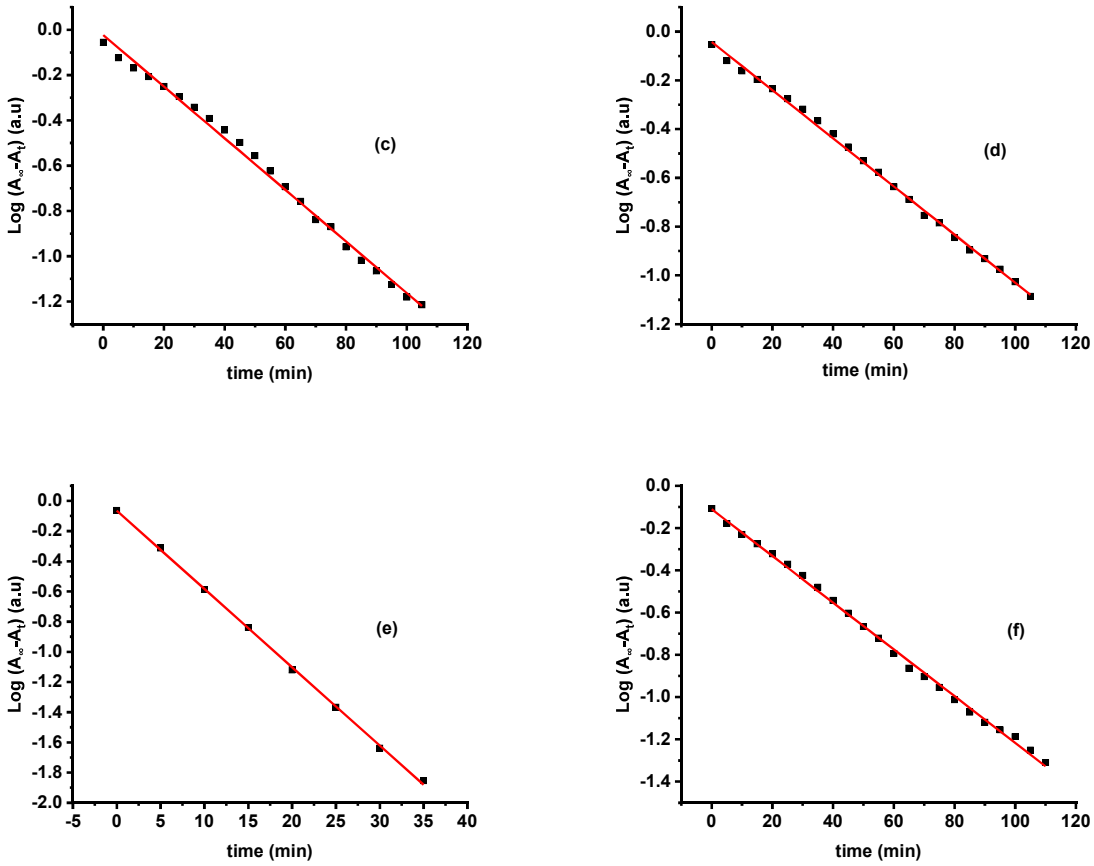


**Figure 2.9**. **(a)** Time-resolved absorption peaks, **(b-f)** Pseudo first-order kinetic plots for the reaction of $6\times10^{-4}$ mol $L^{-1}$ **1b** in $1.1\times10^{-2}$ mol $L^{-1}$ CTAB using $1.8\times10^{-3}$ mol $L^{-1}$ of **(b)** $CuCl_2.2H_2O$, **(c)** $CuSO_4$, **(d)** $CuBr_2$, **(e)** $Cu(OAc)_2$ and **(f)** $Cu(NO_3)_2.3H_2O$, Experimental data (dotted line), solid line fit to the (pseudo) first-order equation (1), at 65˚C

**Figure 2.9 (a)** shows increasing in absorbance at 279nm for **(b-f)** as the reaction proceeds the (4,4'-dimethyl-1,1'-biphenyl) is produced as the only product without phenol. The observed rate constant $k_{obs}$ for the **Figure 2.9** is shown in **Table 2**.

**Table 2.** The observed rate constant $k_{obs}$ for the reaction of **1b** at optimum conditions using different copper catalysts.

| 1b (mol $L^{-1}$) | Cu-catalysts ($1.8\times10^{-3}$ mol $L^{-1}$) | $k_{obs}$ ($min^{-1}$) |
|---|---|---|
| $6\times10^{-4}$ | $Cu(OAc)_2$ | 0.1194 |
| $6\times10^{-4}$ | $CuSO_4$ | 0.0262 |
| $6\times10^{-4}$ | $Cu(NO_3)_2.3H_2O$ | 0.0254 |
| $6\times10^{-4}$ | $CuBr_2$ | 0.0227 |
| $6\times10^{-4}$ | $CuCl_2.2H_2O$ | 0.0183 |

From **Table 1 and Table 2** we can observe that $k_{obs}$ for $Cu(OAc)_2$ are much higher than others, and the observed rate constant $k_{obs}$ for $CuCl_2.2H_2O$ has a minimum value compared to the others. Totally as we compare **Table 1 vs Table 2** we see that the observed rate constant $k_{obs}$ for **1a** in all different copper catalysts are greater than **1b**. This is due to the $(CH_3)$ substituent on the benzene ring in **1b** which will donate electron

through inductive effect to the benzene ring and make it more stable (less reactive) means that react slower than **1a (Smith, 2020).**3.7.2: Homocoupling of 1b using different Copper complex catalysts.

The homocoupling reaction of **1b** is done under mild temperature conditions for (a and b) complexes **Figure 3.**

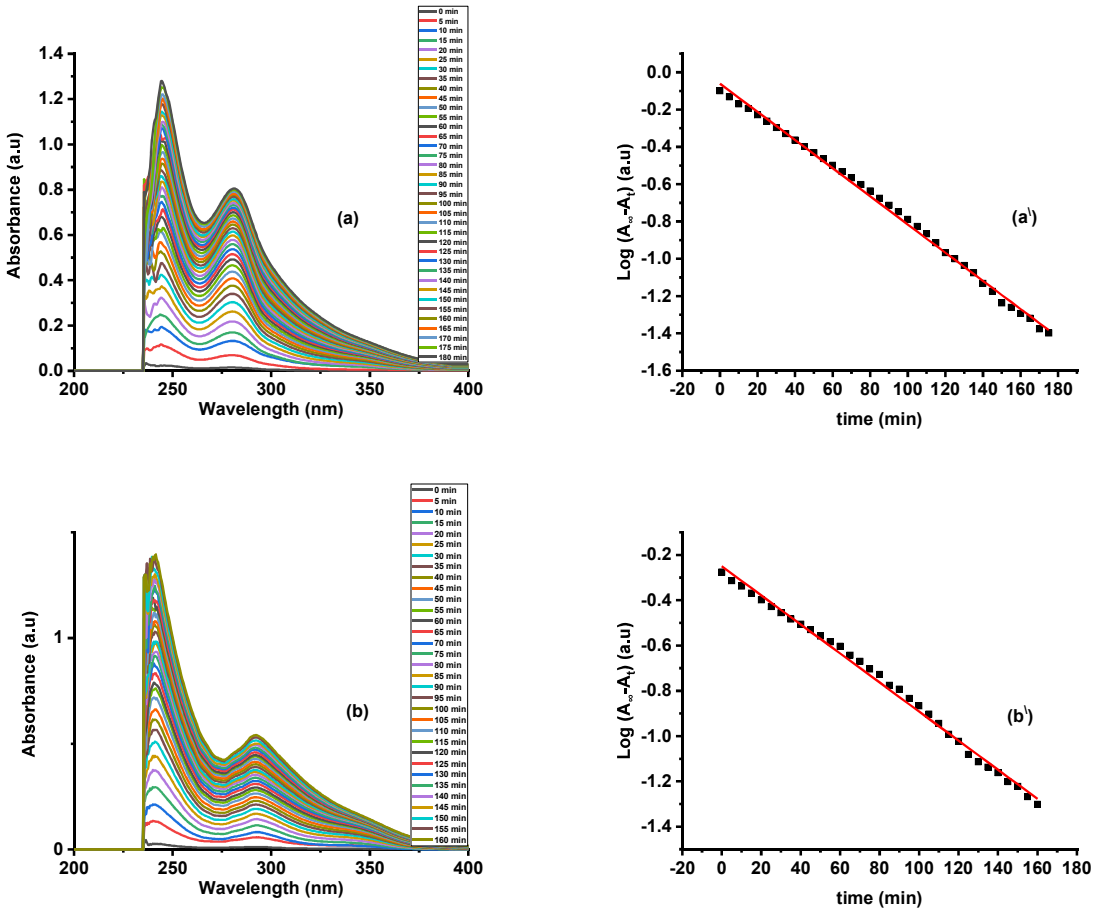


**Figure 3**. **(a,b)** Time-resolved absorption peaks, **(a',b')** Pseudo first-order kinetic plots for the reaction of $6\times10^{-4}$ mol $L^{-1}$ **1b** in $1.1\times10^{-2}$ mol $L^{-1}$ CTAB using $8\times10^{-5}$ mol $L^{-1}$ of **(a)** $[Cu(4\text{-mba})_2(tmeda)]$ and **(b)** $[Cu(3\text{-mba})_2(H_2O)_2(tmeda)]$, **(a',b')** Experimental data (dotted line), solid line fit to the (pseudo) first-order equation (1), at 85˚C, $k_{obs}$=(0.0173, 0.0147 $min^{-1}$) respectively

**Figure 3**. Shows that there is increasing in absorbance for **(a)** $[Cu(4\text{-mba})_2(tmeda)]$ at 281nm while for **(b)** $[Cu(3\text{-mba})_2(H_2O)_2(tmeda)]$ at 292nm as the reaction proceed the (4,4'-dimethyl-1,1'-biphenyl) is produced as the only product without phenol.

Comparing **Figure 2.8 vs Figure 3** we observe that $k_{obs}$ for **(a)** catalyst are nearly the same but for **(b)** is not the same $k_{obs}$ for **1a** using $[Cu(3\text{-mba})_2(H_2O)_2(tmeda)]$ is greater than for **1b**.

### 3.8: Homocoupling of 4-Acetyl phenylboronic acid (1c) using different Copper catalysts.

Under optimized conditions, the homocoupling reaction of **1c** using a different copper catalyst (a-e) is done **Figure 3.1**.

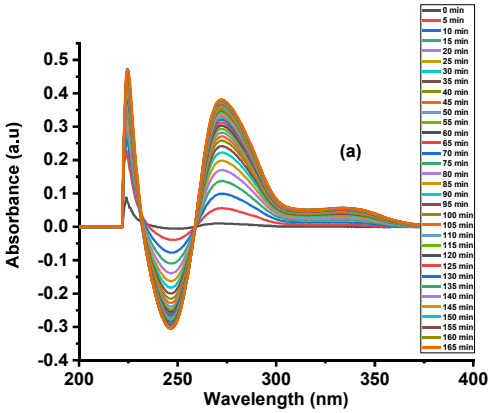
Absorbance (a.u)
Wavelength (nm)
(a)
0 min
5 min
10 min
15 min
20 min
25 min
30 min
35 min
40 min
45 min
50 min
55 min
60 min
65 min
70 min
75 min
80 min
85 min
90 min
95 min
100 min
105 min
110 min
115 min
120 min
125 min
130 min
135 min
140 min
145 min
150 min
155 min
160 min
165 min

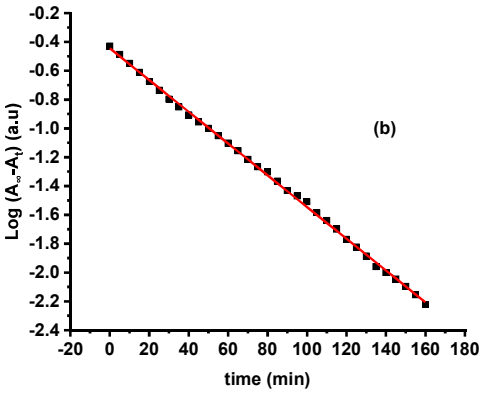
Log (A∞-At) (a.u)
time (min)
(b)

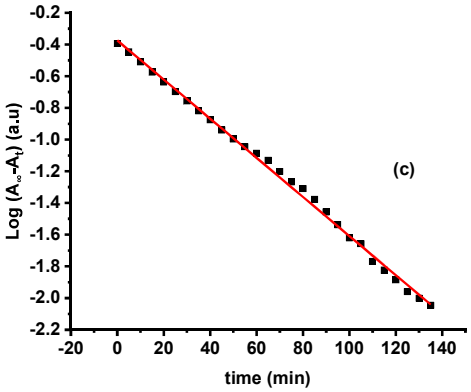
Log (A∞-At) (a.u)
time (min)
(c)

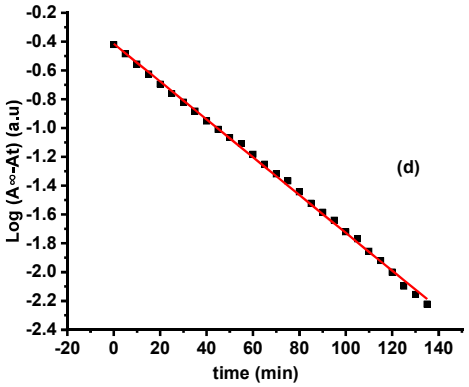
Log (A∞-At) (a.u)
time (min)
(d)

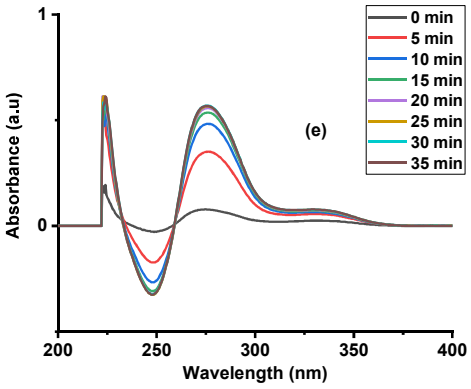
Absorbance (a.u)
Wavelength (nm)
(e)
0 min
5 min
10 min
15 min
20 min
25 min
30 min
35 min

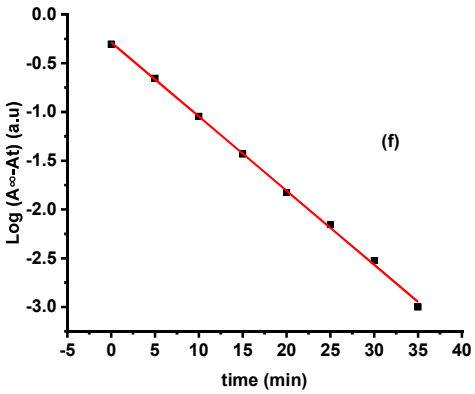
Log (A∞-At) (a.u)
time (min)
(f)

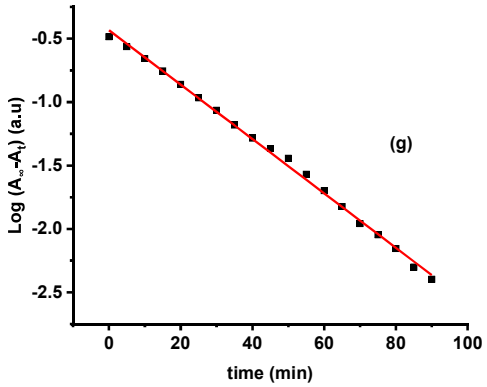


**Figure 3.1**. **(a,e)** Time-resolved absorption peaks, **(b,c,d,f and g)** Pseudo first-order kinetic plots for the reaction of $6\times10^{-5}$ mol $L^{-1}$ **1c** in $1.1\times10^{-2}$ mol $L^{-1}$ CTAB using $1.8\times10^{-3}$ mol $L^{-1}$ of **(b)** $CuCl_2.2H_2O$, **(c)** $CuSO_4$, **(d)** $CuBr_2$, **(f)** $Cu(OAc)_2$ and **(g)** $Cu(NO_3)_2.3H_2O$, Experimental data (dotted line), solid line fit to the (pseudo) first-order equation (1), at 65˚C

**Figure 3.1 (a,e)** show increasing in absorbance at 272nm for **(b,c,d and g)**, and 279nm for **(f)** respectively as the reaction proceed the (1,1'-([1,1'-biphenyl]-4,4'-diol)bis(ethan-1-one)) is produced as the only product without phenol. The $k_{obs}$ for the **Figure 3.1** are shown in **Table 3**.

**Table 3.** The observed rate constant $k_{obs}$ for the reaction of **1c** at optimum conditions using different copper catalysts.

| 1c (mol $L^{-1}$) | Cu-catalysts ($1.8\times10^{-3}$ mol $L^{-1}$) | $k_{obs}$ ($min^{-1}$) |
|---|---|---|
| $6\times10^{-5}$ | $Cu(OAc)_2$ | 0.1808 |
| $6\times10^{-5}$ | $CuSO_4$ | 0.0284 |
| $6\times10^{-5}$ | $Cu(NO_3)_2.3H_2O$ | 0.0493 |
| $6\times10^{-5}$ | $CuBr_2$ | 0.0302 |
| $6\times10^{-5}$ | $CuCl_2.2H_2O$ | 0.0253 |

### 3.9: Homocoupling of 4-Formyl phenylboronic acid (1d) using different Copper catalysts.

Under optimized conditions, the homocoupling reaction of (**1d**) using a different copper catalyst **(a-e)** is done **Figure 3.2**.

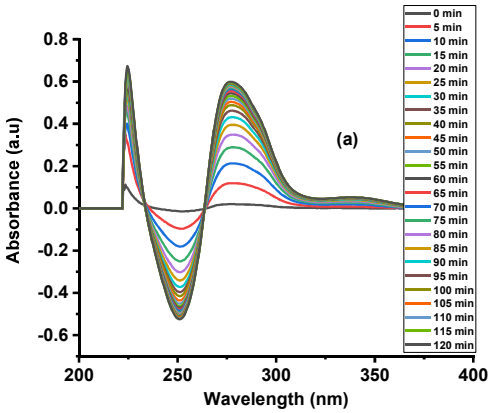
(a)
Absorbance (a.u)
Wavelength (nm)
0 min
5 min
10 min
15 min
20 min
25 min
30 min
35 min
40 min
45 min
50 min
55 min
60 min
65 min
70 min
75 min
80 min
85 min
90 min
95 min
100 min
105 min
110 min
115 min
120 min

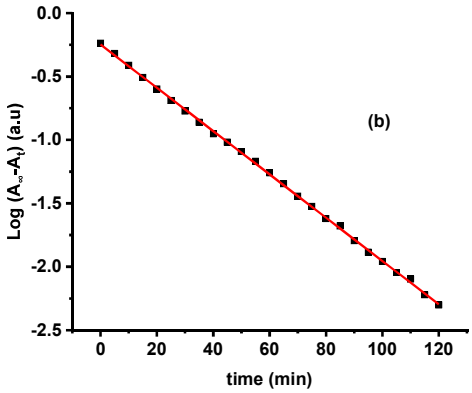
(b)
Log (A∞-At) (a.u)
time (min)

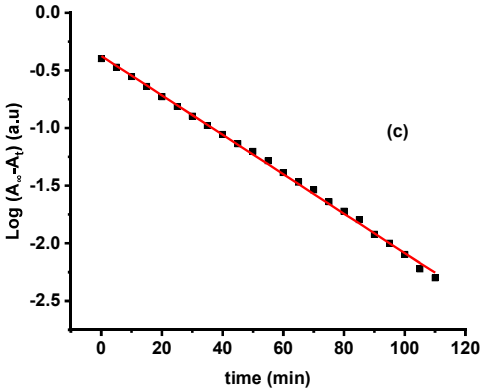
(c)
Log (A∞-At) (a.u)
time (min)

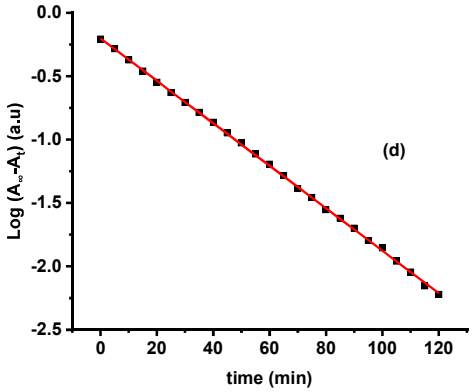
(d)
Log (A∞-At) (a.u)
time (min)

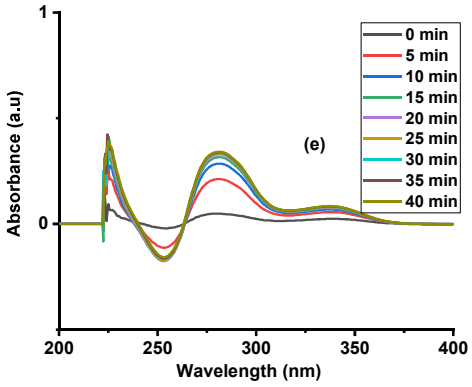
(e)
Absorbance (a.u)
Wavelength (nm)
0 min
5 min
10 min
15 min
20 min
25 min
30 min
35 min
40 min

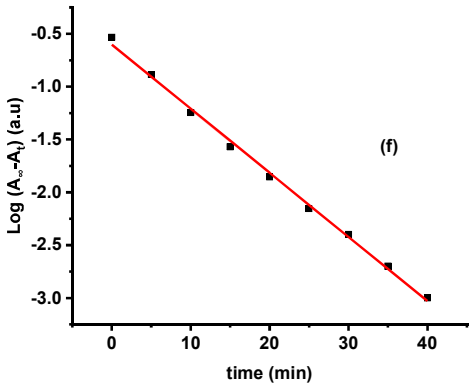
(f)
Log (A∞-At) (a.u)
time (min)

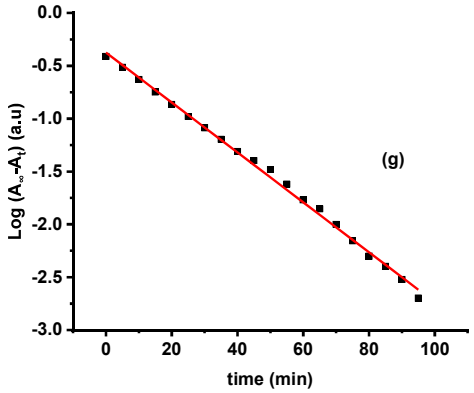


**Figure 3.2**. **(a,e)** Time-resolved absorption peaks, **(b,c,d,f and g)** Pseudo first-order kinetic plots for the reaction of $6\times10^{-5}$ mol $L^{-1}$ **1d** in $1.1\times10^{-2}$ mol $L^{-1}$ CTAB using $1.8\times10^{-3}$ mol $L^{-1}$ of **(b)** $CuCl_2.2H_2O$, **(c)** $CuSO_4$, **(d)** $CuBr_2$, **(f)** $Cu(OAc)_2$ and **(g)** $Cu(NO_3)_2.3H_2O$, Experimental data (dotted line), solid line fit to the (pseudo) first-order equation (1), at 65˚C

**Figure 3.2 (a,e)** shows increasing in absorbance at 277nm for **(b,c,d, and g)** and 282nm for **(f)** respectively as the reaction proceeds the( [1,1'-biphenyl]-4,4'-dicarbaldehyde) is produced as the only product without phenol. The $k_{obs}$ for the **Figure 3.2** are shown in **Table 4**.

**Table 4.** The observed rate constant $k_{obs}$ for the reaction of **1d** at optimum conditions using different copper catalysts.

| 1d (mol $L^{-1}$) | Cu-catalysts ($1.8\times10^{-3}$ mol $L^{-1}$) | $k_{obs}$ ($min^{-1}$) |
|---|---|---|
| $6\times10^{-5}$ | $Cu(OAc)_2$ | 0.1397 |
| $6\times10^{-5}$ | $CuSO_4$ | 0.0394 |
| $6\times10^{-5}$ | $Cu(NO_3)_2.3H_2O$ | 0.0543 |
| $6\times10^{-5}$ | $CuBr_2$ | 0.0385 |
| $6\times10^{-5}$ | $CuCl_2.2H_2O$ | 0.0393 |

From **Tables 1,2,3 and 4** we observe that the $k_{obs}$ for $Cu(OAc)_2$ are much higher than others and the $k_{obs}$ for $CuCl_2.2H_2O$ has a minimum value compared to the others. We can explain that the counter ion acetate anion ($CH_3COO^-$) has a resonance stability effect which causes the delocalization of electron pair (-) charge between two oxygen atoms as shown in **(Scheme 8).**

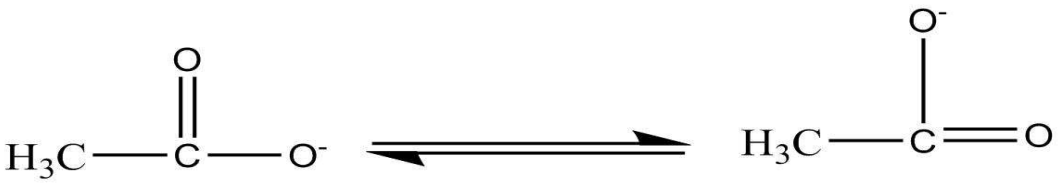


**Scheme 8.** resonance structure of acetate ion.

This will lead to increasing the stability of the acetate anion hence leading to releasing the ($Cu^{2+}$) to be freer to move (reactivity increase) therefore

it will be more catalytically active (Smith, 2020) as a result **Tables of 1,2,3 and 4** all show that the $k_{obs}$ for $Cu(OAc)_2$ are the highest. Therefore, we used it to study the effects of (catalyst concentration, **1a** concentration, CTAB concentration, and temperature) at 40˚C, The chloride and bromide ions have the minimum $k_{obs}$ since they do not have resonance. As we see from **Figures 3.1 and 3.2** we note that there is a decrease in absorbance at 250nm as the reaction proceeds and the absorbance has a negative value which is because of the copper catalyst in addition homocoupling reaction will oxidize the carbonyl group of (**1c** and **1d**) to produce carboxylic acid according to the literature (Liu and Li, 2016) as shown in **(Scheme 9)**.

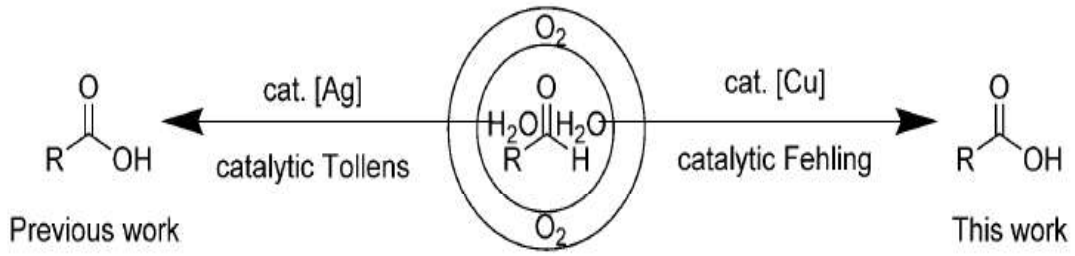


**Scheme 9**. Catalytic aerobic oxidation of aldehydes (Liu and Li, 2016).

## 4. Conclusions

In conclusion, using copper catalysts we were able to successfully study the kinetics of homocoupling of different phenylboronic acids. This approach is advantageous because it allows for the use of cheap copper sources that are widely available. The other benefit of using the copper catalyst is that does not need any additive such as base or oxidant. The UV-Vis spectrophotometer is used to follow the reaction. Pseudo-first-order equation was applied for calculating observed rate constants $k_{obs}$. Among all the copper catalysts used the $Cu(OAc)_2$ was the best catalyst for the kinetic study of homocoupling phenyl boronic acid in an aqueous micellar medium (40˚C temperature, fast reaction rate). The observed rate constant increased as the concentration of CTAB increases until it reaches critical micelle concentration (CMC) $1\times10^{-3}$ mol $L^{-1}$ but when exceeds CMC starts to decline. The observed rate constant increased linearly with catalyst concentration proving that the reaction is first order with respect to the catalyst concentration. Studying the effect **1a** concentration indicated that with increasing the concentration of **1a** the $k_{obs}$ decrease the number of reasons that could be responsible for this drop mainly attributed to $O_2$ the $O_2$ concentration decreases in the reaction mixture and formation of dimerizing or trimerizing of **1a**. The activation energy (**Ea)** was found using the Arrhenius equation by studying the temperature effect on the homocoupling **1a** reaction.

## Acknowledgement

We are gratefully thank Prof. Dr. Bakhtiar Aziz for providing us the homemade cuvette holder. Special thanks go to Mr. Adnan Qadir for providing us with the two copper complexes. Last but not least a huge thank go to Dr. Hunar Othman for his kind help in instrumental lab.

## References

AMATORE, C., CAMMOUN, C. & JUTAND, A. 2008. Pd (OAc) 2/p-Benzoquinone-Catalyzed Anaerobic Electrooxidative Homocoupling of Arylboronic Acids, Arylboronates and Aryltrifluoroborates in DMF and/or Water. Wiley Online Library.

ATKINS, P., ATKINS, P. W. & DE PAULA, J. 2014. *Atkins' physical chemistry*, Oxford university press.

BASNET, P., THAPA, S., DICKIE, D. A. & GIRI, R. 2016. The copper-catalysed Suzuki–Miyaura coupling of alkylboron reagents: disproportionation of anionic (alkyl)(alkoxy) borates to anionic dialkylborates prior to transmetalation. *Chemical Communications,* 52**,** 11072-11075.

BOULEGHLIMAT, A., OTHMAN, M. A., LAGRAVE, L. V., MATSUZAWA, S., NAKAMURA, Y., FUJII, S. & BUURMA, N. J. 2017. Halide-enhanced catalytic activity of palladium nanoparticles comes at the expense of catalyst recovery. *Catalysts,* 7**,** 280.

BURNS, M. J., FAIRLAMB, I. J., KAPDI, A. R., SEHNAL, P. & TAYLOR, R. J. 2007. Simple Palladium (II) Precatalyst for Suzuki– Miyaura Couplings: Efficient Reactions of Benzylic, Aryl, Heteroaryl, and Vinyl Coupling Partners. *Organic letters,* 9**,** 5397-5400.

BUURMA, N. J. 2009. Kinetic medium effects on organic reactions in aqueous colloidal solutions. *Advances in Physical Organic Chemistry,* 43**,** 1-37.

CAO, Y.-N., TIAN, X.-C., CHEN, X.-X., YAO, Y.-X., GAO, F. & ZHOU, X.-L. 2017. Rapid Ligand-Free Base-Accelerated Copper-Catalyzed Homocoupling Reaction of Arylboronic Acids. *Synlett,* 28**,** 601-606.

CHENG, G. & LUO, M. 2011. Homocoupling of arylboronic acids catalyzed by CuCl in air at room temperature. Wiley Online Library.

CHENG, K., XIN, B. & ZHANG, Y. 2007. The Pd (OAc) 2-catalyzed homocoupling of arylboronic acids in water and ionic liquid. *Journal of Molecular Catalysis A: Chemical,* 273**,** 240-243.

CICCO, S. R., FARINOLA, G. M., MARTINELLI, C., NASO, F. & TIECCO, M. 2010. Pd-Promoted Homocoupling Reactions of Unsaturated Silanes in Aqueous Micelles. Wiley Online Library.

CORBET, J.-P. & MIGNANI, G. 2006. Selected patented cross-coupling reaction technologies. *Chemical reviews,* 106**,** 2651-2710.

DAR, B. A., SINGH, S., PANDEY, N., SINGH, A., SHARMA, P., LAZAR, A., SHARMA, M., VISHWAKARMA, R. A. & SINGH, B. 2014. Clay encapsulated Cu (OH) x promoted homocoupling of arylboronic acids: An efficient and eco-friendly protocol. *Applied Catalysis A: General,* 470**,** 232-238.

DEMIR, A. S., REIS, Ö. & EMRULLAHOGLU, M. 2003. Role of copper species in the oxidative dimerization of arylboronic acids: Synthesis of symmetrical biaryls. *The Journal of organic chemistry,* 68**,** 10130-10134.

GALLON, B. J., KOJIMA, R. W., KANER, R. B. & DIACONESCU, P. L. 2007. Palladium nanoparticles supported on polyaniline nanofibers as a semi-heterogeneous catalyst in water. *Angewandte Chemie International Edition,* 46**,** 7251-7254.

GRATZEL, M. 2020. *Kinetics and catalysis in microheterogeneous systems*, CRC Press.

HORTON, D. A., BOURNE, G. T. & SMYTHE, M. L. 2003. The combinatorial synthesis of bicyclic privileged structures or privileged substructures. *Chemical reviews,* 103**,** 893-930.

JIN, Z., GUO, S. X., GU, X. P., QIU, L. L., SONG, H. B. & FANG, J. X. 2009. Highly Active, Well-Defined (Cyclopentadiene)(N-heterocyclic carbene) palladium Chloride Complexes for Room-Temperature Suzuki–Miyaura and Buchwald–Hartwig Cross-Coupling Reactions of Aryl Chlorides and Deboronation Homocoupling of Arylboronic Acids. *Advanced Synthesis & Catalysis,* 351**,** 1575-1585.

KABALKA, G. W. & WANG, L. 2002. Ligandless palladium chloride-catalyzed homo-coupling of arylboronic acids in aqueous media. *Tetrahedron letters,* 43**,** 3067-3068.

KABOUDIN, B., ABEDI, Y. & YOKOMATSU, T. 2011a. CuII–β-Cyclodextrin Complex as a Nanocatalyst for the Homo-and Cross-Coupling of Arylboronic Acids under Ligand-and Base-Free Conditions in Air: Chemoselective Cross-Coupling of Arylboronic Acids in Water. Wiley Online Library.

KABOUDIN, B., HARUKI, T. & YOKOMATSU, T. 2011b. CuSO4-mediated homocoupling of arylboronic acids under ligand-and base-free conditions in air. *Synthesis,* 2011**,** 91-96.

KANSıZ, S., QADIR, A. M., DEGE, N. & FAIZI, S. H. 2021. Two new copper (II) carboxylate complexes based on N, N, N', N'-tetramethylethyleneamine: Synthesis, crystal structures, spectral properties, dft studies and hirshfeld surface analysis. *Journal of Molecular Structure,* 1230**,** 129916.

KARIMI, B. & AKHAVAN, P. F. 2009. Main-chain NHC-palladium polymer as a recyclable self-supported catalyst in the Suzuki–Miyaura coupling of aryl chlorides in water. *Chemical communications***,** 3750-3752.

KHALILY, M. A., USTAHUSEYIN, O., GARIFULLIN, R., GENC, R. & GULER, M. O. 2012. A supramolecular peptide nanofiber templated Pd nanocatalyst for efficient Suzuki coupling reactions under aqueous conditions. *Chemical Communications,* 48**,** 11358-11360.

KIRAI, N. & YAMAMOTO, Y. 2009. Homocoupling of Arylboronic Acids Catalyzed by 1, 10-Phenanthroline-Ligated Copper Complexes in Air. Wiley Online Library.

KLINGENSMITH, L. M. & LEADBEATER, N. E. 2003. Ligand-free palladium catalysis of aryl coupling reactions facilitated by grinding. *Tetrahedron letters,* 44**,** 765-768.

LIU, M. & LI, C. J. 2016. Catalytic Fehling's reaction: an efficient aerobic oxidation of aldehyde catalyzed by copper in water. *Angewandte Chemie,* 128**,** 10964-10968.

LLOYD-WILLIAMS, P. & GIRALT, E. 2001. Atropisomerism, biphenyls and the Suzuki coupling: peptide antibioticsAbbreviations: Bn= benzyl; Boc= tert-butoxycarbonyl; dba= dibenzylideneacetone; Ddm= 4, 4′-dimethoxydiphenylmethyl; DMSO= dimethylsulfoxide; FDPP= pentafluorophenyl diphenylphosphinate; MEM= methoxyethoxymethyl; Ms= methylsulfonyl; Piv= pivaloyl; TBS= tert-butyldimethylsilyl; Tf= trifluoromethanesulfonyl; Tfa= trifluoroacetyl; TFA= trifluoroacetic acid; Z= benzoxycarbonyl. *Chemical Society Reviews,* 30**,** 145-157.

MARIN, G. 2011. G. Yablonsky'Kinetics of Complex Reactions. Decoding Complexity'. J. Wiley-VCH.

MARION, N., NAVARRO, O., MEI, J., STEVENS, E. D., SCOTT, N. M. & NOLAN, S. P. 2006. Modified (NHC) Pd (allyl) Cl (NHC= N-heterocyclic carbene) complexes for room-temperature Suzuki–Miyaura and Buchwald–Hartwig reactions. *Journal of the American Chemical Society,* 128**,** 4101-4111.

MARTIN, R. & BUCHWALD, S. L. 2008. Palladium-catalyzed Suzuki– Miyaura cross-coupling reactions employing dialkylbiaryl phosphine ligands. *Accounts of chemical research,* 41**,** 1461-1473.

MCGLACKEN, G. P. & BATEMAN, L. M. 2009. Recent advances in aryl–aryl bond formation by direct arylation. *Chemical Society Reviews,* 38**,** 2447-2464.

MITSUDO, K., SHIRAGA, T., KAGEN, D., SHI, D., BECKER, J. Y. & TANAKA, H. 2009. Pd/TEMPO-catalyzed electrooxidative synthesis of biaryls from arylboronic acids or arylboronic esters. *Tetrahedron,* 65**,** 8384-8388.

MITSUDO, K., SHIRAGA, T. & TANAKA, H. 2008. Electrooxidative homo-coupling of arylboronic acids catalyzed by electrogenerated cationic palladium catalysts. *Tetrahedron Letters,* 49**,** 6593-6595.

MIYAURA, N. & SUZUKI, A. 1995. Palladium-catalyzed cross-coupling reactions of organoboron compounds. *Chemical reviews,* 95**,** 2457-2483.

MONNIER, F. & TAILLEFER, M. 2009. Catalytic C□ C, C□ N, and C□ O Ullmann-Type Coupling Reactions. *Angewandte Chemie International Edition,* 48**,** 6954-6971.

MU, B., LI, T., FU, Z. & WU, Y. 2009. Cyclopalladated ferrocenylimines catalyzed-homocoupling reaction of arylboronic acids in aqueous solvents at room temperature under ambient atmosphere. *Catalysis Communications,* 10**,** 1497-1501.

OTHMAN, M. A. 2011. *Palladium-catalysed aerobic oxidative homocoupling reaction of arylboronic acids in aqueous micellar medium: Kinetic and mechanistic studies*, Cardiff University (United Kingdom).

OTHMAN, M. A. 2020. Stability of Palladium (II) beta-cyclodextrin nanocomposite in aqueous media and its catalytic activity in Homocoupling of Arylboronic acid. *Zanco Journal of Pure and Applied Sciences,* 32**,** 114-121.

PARRISH, J. P., JUNG, Y. C., FLOYD, R. J. & JUNG, K. W. 2002. Oxidative dimerization: Pd (II) catalysis in the presence of oxygen using aqueous media. *Tetrahedron letters,* 43**,** 7899-7902.

PARSHAMONI, S., TELANGAE, J., SANDA, S. & KONAR, S. 2016. A Copper-Based Metal–Organic Framework Acts as a Bifunctional Catalyst for the Homocoupling of Arylboronic Acids and Epoxidation of Olefins. *Chemistry–An Asian Journal,* 11**,** 540-547.

POURMORTEZA, N., JAFARPOUR, M., FEIZPOUR, F. & REZAEIFARD, A. 2022. Cu (ii)–vitamin C-complex catalyzed photo-induced homocoupling reaction of aryl boronic acid in base-free and visible light conditions. *RSC advances,* 12**,** 4931-4938.

PRASTARO, A., CECI, P., CHIANCONE, E., BOFFI, A., CIRILLI, R., COLONE, M., FABRIZI, G., STRINGARO, A. & CACCHI, S. 2009. Suzuki-Miyaura cross-coupling catalyzed by protein-stabilized palladium nanoparticles under aerobic conditions in water: application to a one-pot chemoenzymatic enantioselective synthesis of chiral biaryl alcohols. *Green Chemistry,* 11**,** 1929-1932.

PRASTARO, A., CECI, P., CHIANCONE, E., BOFFI, A., FABRIZI, G. & CACCHI, S. 2010. Homocoupling of arylboronic acids and potassium aryltrifluoroborates catalyzed by protein-stabilized palladium nanoparticles under air in water. *Tetrahedron Letters,* 51**,** 2550-2552.

PUTHIARAJ, P., SURESH, P. & PITCHUMANI, K. 2014. Aerobic homocoupling of arylboronic acids catalysed by copper terephthalate metal–organic frameworks. *Green Chemistry,* 16**,** 2865-2875.

RAUL, P. K., MAHANTA, A., BORA, U., THAKUR, A. J. & VEER, V. 2015. In water homocoupling of arylboronic acids using nano-rod shaped and reusable copper oxide (II) catalyst at room temperature. *Tetrahedron letters,* 56**,** 7069-7073.

SCRIMIN, P., TECILLA, P., TONELLATO, U. & BUNTON, C. A. 1998. Nucleophilic catalysis of hydrolyses of phosphate and carboxylate esters by metallomicelles: facts and misconceptions. *Colloids and Surfaces A: Physicochemical and Engineering Aspects,* 144**,** 71-79.

SMITH, M. B. 2020. *March's advanced organic chemistry: reactions, mechanisms, and structure*, John Wiley & Sons.

VAN OS, N. M., HAAK, J. R. & RUPERT, L. A. M. 2012. *Physico-chemical properties of selected anionic, cationic and nonionic surfactants*, Elsevier.

WONG, M. S. & ZHANG, X. L. 2001. Ligand promoted palladium-catalyzed homo-coupling of arylboronic acids. *Tetrahedron Letters,* 42**,** 4087-4089.

YADAV, J. S., GAYATHRI, K. U., ATHER, H., UR REHMAN, H. & PRASAD, A. R. 2007. Utility of semicarbazones as ligands in newly made palladium complex for facile Suzuki homocoupling reaction of alkyl and aryl boronic acids. *Journal of Molecular Catalysis A: Chemical,* 271**,** 25-27.

YAMAMOTO, Y. 2007. Homocoupling of arylboronic acids with a catalyst system consisting of a palladium (II) N-heterocyclic carbene complex and p-benzoquinone. *Synlett,* 2007**,** 1913-1916.

YAMAMOTO, Y., SUZUKI, R., HATTORI, K. & NISHIYAMA, H. 2006. Base-and phosphine-free palladium-catalyzed homocoupling of arylboronic acid derivatives under air. *Synlett,* 2006**,** 1027-1030.

YANG, X.-F., ZHANG, L.-L. & ZHU, H.-B. 2021a. Size-Selective Homocoupling of Arylboronic Acids Mediated by a Copper-Based Metal–Organic-Framework. *Journal of Inorganic and Organometallic Polymers and Materials,* 31**,** 4623-4627.

YANG, X.-F., ZHANG, L.-L. & ZHU, H.-B. 2021b. Size-Selective Homocoupling of Arylboronic Acids Mediated by a Copper-Based Metal–Organic-

Framework. *Journal of Inorganic and Organometallic Polymers and Materials*, 1-5.

YUAN, C., ZHENG, L. & ZHAO, Y. 2019. Cu (II)-Catalyzed Homocouplings of (Hetero) Arylboronic Acids with the Assistance of 2-O-Methyl-d-Glucopyranose. *Molecules,* 24, 3678.

ZHOU, L., XU, Q. X. & JIANG, H. F. 2007. Palladium-catalyzed homo-coupling of boronic acids with supported reagents in supercritical carbon dioxide. *Chinese Chemical Letters,* 18, 1043-1046.